ACS APPLIED MATERIALS & INTERFACES

Research Article

www.acsami.org

# Biocomposites from Natural Rubber: Synergistic Effects of Functionalized Cellulose Nanocrystals as Both Reinforcing and Cross-Linking Agents via Free-Radical Thiol−ene Chemistry

Bipinbal Parambath Kanoth,[†] Mauro Claudino,[‡] Mats Johansson,[†,‡] Lars A. Berglund,[†,‡] and Qi Zhou*[,†,§]

[†]Wallenberg Wood Science Center, Royal Institute of Technology, 100 44 Stockholm, Sweden

[‡]Department of Fibre and Polymer Technology, Royal Institute of Technology, 100 44 Stockholm, Sweden

[§]School of Biotechnology, AlbaNova University Centre, Royal Institute of Technology, 106 91 Stockholm, Sweden

**ABSTRACT:** Natural rubber/cellulose nanocrystals (NR/CNCs) form true biocomposites from renewable resources and are demonstrated to show significantly improved thermo-mechanical properties and reduced stress-softening. The nanocomposites were prepared from chemically functionalized CNCs bearing thiols. CNCs served as both reinforcing and cross-linking agents in the NR matrix, and the study was designed to prove the cross-linking function of modified CNCs. CNCs were prepared from cotton, and the cross-linkable mercapto-groups were introduced onto the surface of CNCs by esterification. Nanocomposite films were prepared by dispersing the modified CNCs (m-CNCs) in NR matrix by solution casting. The cross-links at the filler−matrix (m-CNCs−NR) interface were generated by photochemically initiated thiol−ene reactions as monitored by real-time FTIR analysis. The synergistic effects of reinforcement and chemical cross-linking at the m-CNCs−NR interface on structure, thermo-mechanical, and stress-softening behavior were investigated. Methods included field emission scanning electron microscopy (FE-SEM), swelling tests, dynamic mechanical analysis, and tensile tests. Compared to biocomposites from NR with unmodified CNCs, the NR/m-CNCs nanocomposites showed 2.4-fold increase in tensile strength, 1.6-fold increase in strain-to-failure, and 2.9-fold increase in work-of-fracture at 10 wt % of m-CNCs in NR.

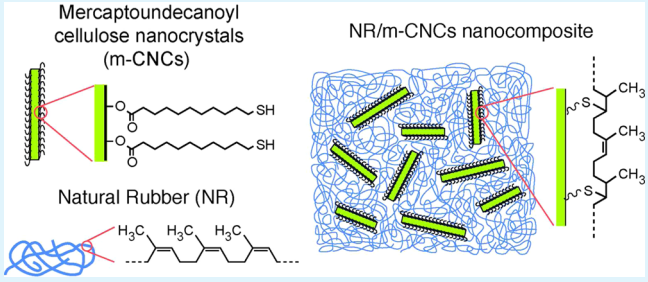


**KEYWORDS:** *cellulose nanocrystals, natural rubber, thiol−ene chemistry, nanocomposites, interface, mechanical properties*

## INTRODUCTION

Natural rubber (NR) is one of the most important elastomers in terms of versatility and application volume owing to its superior strength, elasticity, flexibility, resilience, and abrasion resistance. Natural rubber is a high molecular weight biopolymer of isoprene (2-methyl 1,3-butadiene). It is traditionally vulcanized using sulfur or sulfur compounds due to its low strength and poor weather resistance in original uncured form. During vulcanization, sulfide linkages are formed between linear natural rubber molecules, resulting in the formation of a three-dimensional network structure.[1] This is essential for generating the elastomeric properties of natural rubber combined with good thermal stability and barrier properties. Significant progress has been made in other chemical and physical techniques for rubber cross-linking.[2,3] Further improvement in mechanical properties of natural rubber can be achieved by the addition of reinforcing fillers, such as carbon black[4] and silica.[5,6] Carbon black produced from petroleum oil is carcinogenic and about 90% of the worldwide production of carbon black is used as reinforcing filler in the tire industry. To reduce the health hazards and environmental issues associated with production and application of tires, the use of carbon black has to be reduced through substitution with more eco-friendly components.

Tremendous efforts have already been made to produce eco-friendly tires, either by reducing the rolling resistance of tires which reduces fuel consumption and minimizes emissions or by reducing the concentration of petroleum-based materials in tires. Major tire manufacturers, Michelin, Pirelli, and Bridgestone, have replaced part of the carbon black with silica to reduce rolling resistance. Yokohama and Michelin have used vegetable oils in some of their tire formulations instead of petroleum-derived mineral oils. Goodyear used corn-starch derived fillers in partial replacement of carbon black and silica.[7,8]

There has been a recent surge in the research and development of nanostructured elastomer composites, in which the reinforcing fillers are of nanoscale. The large specific surface area of the nanofillers is instrumental in imparting improved properties at lower volume fractions, compared to macro or micro particles. Much stronger reinforcing effect in

**Received:** April 10, 2015
**Accepted:** July 7, 2015
**Published:** July 7, 2015





DOI: 10.1021/acsami.5b03115
*ACS Appl. Mater. Interfaces* 2015, 7, 16303−16310

natural rubber composites has been achieved by using nanoscale fillers such as carbon nanotubes[9] and layered silicates.[10−12] There has been a growing interest to improve the performance of composites using reinforcements derived from renewable resources. Nanocelluloses, cellulose nanoparticles with one dimension in the nanometer range, have been successfully isolated from different raw cellulose resources by using various processing approaches.[13,14] Nanocelluloses including cellulose nanocrystals or nanofibrils were incorporated as reinforcing filler in a nonvulcanized rubber matrix.[15−17] The rubber matrix and cellulose nanoparticles are incompatible, and the molecular scale interactions between them are not sufficient to produce a satisfactory enhancement in properties. Moreover, the agglomerates of cellulose nanoparticles lead to poor dispersion of them in the rubber matrix and act as points of stress concentration, resulting in low strain failure of the composites. Nanocomposites were also prepared with a cross-linked rubber matrix using sulfur as the vulcanizing agent.[18−20] The improvement in mechanical properties of the composites by the addition of nanocelluloses was not very high, as expected due to insufficient interfacial adhesion and interaction between the reinforcements and the matrix. To improve the compatibility between nanocelluloses and rubbery matrix, Rosilo et al.[21] modified cellulose nanocrystals (CNCs) surfaces with a hydrocarbon chain with a double bond at the chain end. A bifunctional dithiol cross-linker was then used with a UV-initiator to create covalent bonds at the interface between modified CNCs and the polybutadiene (PBD) matrix by means of a thiol−ene reaction[22] triggered by UV radiation. The resulting composites showed increased mechanical properties owing to the intercalated structures of alternating reinforcing modified CNCs and rubbery PBD. Indeed, internal trisubstituted double bonds have been demonstrated to retain enough reactivity for the thiol−ene coupling process via a free-radical mechanism.[23−25] Using cellulose nanoparticle as the cross-linking agent, Goetz et al.[26,27] developed cross-linked cellulose whisker nanocomposites using poly(methyl vinyl ether-*co*-maleic acid)−polyethylene glycol as the matrix. The cross-linking via an esterification reaction between cellulose and the matrix prevented nanowhisker aggregation by trapping the nanowhiskers in the cross-linked network and produced nanocomposites with unique mechanical behavior. In our previous work,[28] we have demonstrated that the reinforcing CNCs also act as chemically functional cross-linking sites in a polyurethane elastomer network, resulting in remarkably enhanced thermal and mechanical properties. Thus, both the dispersion of nanofillers in the polymer matrices and the chemistry at the nanofiller−matrix interface are important to the properties of the nanocomposites.

Here, we explore the potential of using CNCs not only as the reinforcing filler but also as the cross-linking reagent in the biobased natural rubber matrix. To achieve a synergistic effect of reinforcement and cross-linking at the interface, CNCs surfaces are modified by surface-grafted brushes using a long hydrocarbon chain with thiol (−SH) groups at the end. Nanocomposites are prepared by solution casting with modified CNCs dispersed in natural rubber. Covalent cross-links are formed between the double bonds of natural rubber molecules and the thiol groups by a photochemically initiated thiol−ene reaction. Note that the nanocomposite is designed to investigate the concept of the formation of covalent cross-links at the interface between CNCs and NR matrix and the corresponding effects on properties, rather than to maximize nanocomposite properties. For better properties, cross-linking chemistry should be used for the NR network itself, e.g., using dithiols such as 1,9-nonanedithiol as the cross-linker[21] or the conventional vulcanizing agents.[19] The structure and thermo-mechanical properties of the nanocomposites are investigated using spectroscopic and thermal methods, scanning electron microscopy, and the tensile mechanical test.

## EXPERIMENTAL SECTION

**Materials.** Natural rubber (grade ISNR 5) was obtained from Rubber Research Institute of India. Cellulose nanocrystals (CNCs) were prepared from cotton cellulose by sulfuric acid hydrolysis according to our previous work.[29] 11-Mercaptoundecanoic acid and acetic anhydride were purchased from Sigma-Aldrich. Glacial acetic acid, concentrated sulfuric acid (95−97%), and toluene were purchased from Fisher Scientific. All these chemicals were used without further purification.

**Preparation of Mercaptoundecanoyl CNCs.** The thiol-modification of CNCs was achieved by esterification according to the method reported previously for thiol-modified cellulose fabrics.[30] 5.212 g of mercaptoundecanoic acid was mixed with 2 mL of acetic anhydride, 0.48 mL of glacial acetic acid, and 0.01 mL of concentrated sulfuric acid in a round-bottom flask and cooled to room temperature. 0.5 g of CNCs was then added and kept in an oil bath at 40 °C for 3 days with magnetic stirring. The thiol-modified CNCs, i.e., mercaptoundecanoyl CNCs (m-CNCs), were precipitated and washed with methanol and finally solvent exchanged to toluene to obtain a stable suspension.

The amount of mercapto groups (thiol content) in the m-CNCs sample was determined by using a colorimetric method.[31] 4 mg of Ellman's reagent (5,5′-dithiobis(2-nitrobenzoic acid)) was dissolved in 1 mL of pH 8.0 phosphate buffer. 5 mg of dry m-CNCs sample was suspended in 2.5 mL of pH 8.0 phosphate buffer in a test tube. 50 μL of 4 mg/mL Ellman's reagent solution was then added and incubated at room temperature for 15 min. The thiol content was determined from the absorbance at 412 nm of the solution using a standard curve derived from cysteine.

**Preparation of NR/m-CNCs Nanocomposites.** Different amounts of 0.5 wt % m-CNCs suspension in toluene were added to a toluene solution of natural rubber (NR) in order to obtain NR/m-CNCs composites with a final m-CNCs content of 2, 5, and 10 wt %. Photoinitiator (Irgacure 651/DMPA) dissolved in toluene was then added to the suspension, and the amount of photoinitiator was kept at 4 wt % of NR. Extra toluene was added to keep the same solution volume in all the composite mixtures. After stirring for 1 h, the mixtures were casted in aluminum dishes and the solvent was evaporated slowly. The casted composite films were finally dried in vacuum and cross-linked by UV irradiation using a UV Fusion Conveyor MC6R equipped with fusion electrodeless bulbs standard type BF9 (UV-fusion lamp). The casted films were passed through the conveyor 35 times. The UV-light intensity was determined with a calibrated radiometer (UVICUREPlus, ET, Sterling, VA). NR/CNCs composite films from unmodified CNCs and neat NR film were prepared in the same way. The samples were coded as NR, NR/CNCs-X, and NR/m-CNCs-X, where X is the weight fraction of the unmodified and modified CNCs in the composites.

**Fourier Transform Infrared Spectroscopy.** Time-resolved Fourier transform infrared (RT-FTIR) spectra were recorded with a PerkinElmer Spectrum 2000 (Norwalk, CT) using an MCT detector cooled with liquid nitrogen. The FTIR instrument was equipped with a heat-controlled Golden Gate single reflection ATR accessory from Graseby Specac (Kent, England). The horizontal ATR sampling unit was modified to accommodate a vertical UV light cable. All FTIR measurements were performed in the reflection mode via the single-bounce diamond ATR crystal. A Hamamatsu L5662 equipped with a standard medium-pressure 200W L6722-01 Hg−Xe lamp and provided with optical fibers was used as the UV-source for the photo-RTIR measurements. A condenser lens adapter, model A4093 from Hamamatsu, was used to focus the UV beam. The height of the


DOI: 10.1021/acsami.5b03115
ACS Appl. Mater. Interfaces 2015, 7, 16303−16310

UV source from the ATR crystal was adjusted to obtain a constant irradiance of 65 mW $cm^{-2}$. The UV intensity was measured using a Hamamatsu UV-light power meter (model C6080-03) calibrated for the main emission line centered at 365 nm.

Conventional ATR-FTIR measurements were performed on a PerkinElmer Spectrum 2000 equipped with a TGS detector using the Golden Gate setup. Each spectrum collected was based on 16 scans averaged at a resolution of 4.0 $cm^{-1}$ in the range of 600−4000 $cm^{-1}$.

**Scanning Electron Microscopy.** Field-emission scanning electron microscopy (FE-SEM) was conducted with a Hitachi S-4800 SEM working at low acceleration voltage (1 kV) and short working distance (8 mm). The frozen sample was quickly cut by a microtome and then coated with a thin layer of platinum/palladium using a sputter coater (Cressington 208HR).

**Dynamic Mechanical Analysis.** Dynamic mechanical analysis (DMA) was performed on a Q800 DMA (TA Instruments), equipped with a film in tension mode fixture. DMA measurements were performed on rectangular samples of 5 mm in width, 30 mm in length, and 100−150 $\mu$m in thickness. All tests were conducted in a temperature range of −80 to +40 °C at a frequency of 1 Hz with a heating rate of 3 °C/min and an oscillating amplitude of 15 $\mu$m.

**Cross-Link Density.** The procedure to measure the cross-link density was as follows: The samples were cut into specimens with a size of 10 × 5 $mm^2$. The dry samples were weighed before soaking in toluene. Swollen samples were periodically taken out from toluene, wiped with a tissue paper, and weighed. The weight measurements were continued until the samples acquired constant weight.

The cross-link density ($\upsilon$) was calculated from the Flory−Rehner equation,[32]

$$\upsilon = \frac{\ln(1 - V_R) + V_R + x_1 V_R^{\,2}}{V_1\left(V_R^{\,1/3} - \frac{V_R}{2}\right)}$$

where

$$V_R = \frac{\frac{W_d}{\rho_d}}{\frac{W_d}{\rho_d} + \frac{W_{sol}}{\rho_{sol}}}$$

$V_1$ and $x_1$ are the molar volume and interaction parameter of solvent (for toluene, $V_1$ = 87.5 mol $cm^{-3}$ and $x_1$ = 0.39), respectively. $W_d$ and $\rho_d$ are the weight and density of rubber ($\rho_d$ = 0.93g $cm^{-3}$), and $W_{sol}$ and $\rho_{sol}$ are the weight and density of solvent (for toluene, $\rho_{sol}$ = 0.865g$cm^{-3}$), respectively.

**Tensile Test.** The mechanical properties of the composites were measured with a universal testing machine (Instron 5944, U.K.), using a 500 N load cell. The measurements were conducted at 50% relative humidity and 22 °C, using specimens of 50 mm in length, 100−150 $\mu$m in thickness, and 5 mm in width with a strain rate of 250 mm/min. The samples were conditioned in the measuring environment for 24 h. The modulus was determined at 5% strain. For stress softening measurements, a strain rate of 100 mm/min was used. Stress−strain responses of 5 cycles were recorded in uniaxial tension with a strain increase of 50% after each cycle.

## RESULTS AND DISCUSSION

**Structure of the NR/m-CNCs Nanocomposite.** Previously, mercapto group (SH) has been incorporated into cellulose derivatives by mercaptoethylation with ethylene sulfide[33] or by esterification with mercaptoacetic acid.[34] Cotton cellulose fibers or fabrics that were surface esterified with mercaptoacetic acid have been used for the synthesis of cellulose-metal nanoparticle composites.[30,35] In this study, we have covalently incorporated the cross-linkable mercapto group on the surface of CNCs by esterification with 11-mercaptoundecanoic acid. Figure 1 shows the FTIR spectra of unmodified CNCs and mercaptoundecanoyl CNCs (m-CNCs). A strong signal at 1743 $cm^{-1}$ in the spectrum of m-CNCs, corresponding

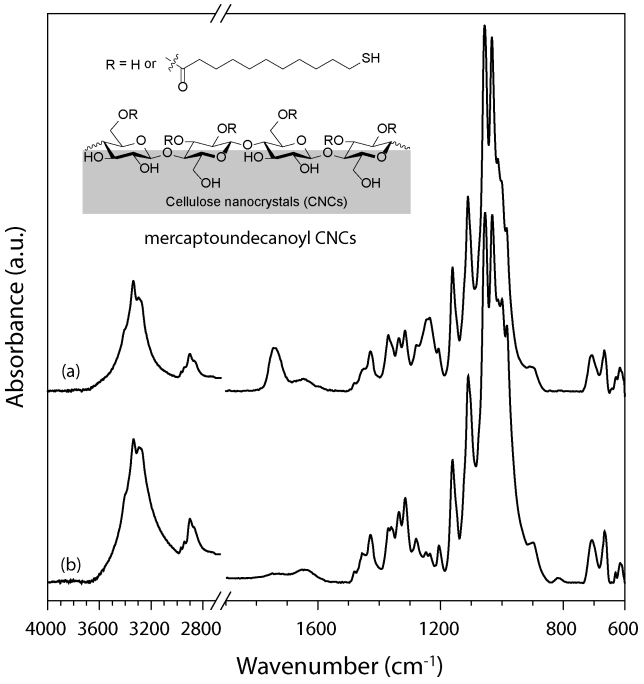


**Figure 1.** FT-IR spectra of the (a) mercaptoundecanoyl CNCs (m-CNCs) and (b) unmodified CNCs.

to the stretching of ester carbonyl group, confirms the success of the esterification reaction leading to the introduction of mercapto groups on the surface of the CNCs. Further evidence for the thiol modification of CNCs was obtained by quantitative analysis of mercapto groups on the nanocrystal surface by a reaction with 5,5′-dithiobis(2-nitrobenzoic acid). The amount of mercapto groups on the m-CNCs was 0.85 mmol/g cellulose as determined by UV−visible spectrophotometry from the amount of 5-thio-2-nitrobenzoic acid anion that was released from the reaction of m-CNCs with 5,5′-dithiobis(2-nitrobenzoic acid). In Figure 2a, a smooth and rather homogeneous surface structure of the cross section of the NR/m-CNCs-10 nanocomposite film is presented, similar to that for the pure NR film (Figure 2c) and vulcanized NR/cellulose nanowhiskers nanocomposites reported previously by Visakh et al.[19] The long hydrocarbon chain on the surface of m-CNCs reduces the hydrophilic nature of the CNCs and improves their compatibility with the hydrophobic natural rubber matrix. Thus, m-CNCs are randomly oriented and homogeneously distributed in the NR matrix. However, the cellulose nanocrystals are hardly distinguished since there is no contrast between the two organic components in the electron microscopy imaging. For the unmodified CNCs in the NR/CNCs-10 nanocomposite, strong phase separation and aggregation is observed (Figure 2b). The unmodified CNCs apparently formed precipitating agglomerates during solution casting on the aluminum dish. Such gradient formation was also observed in earlier studies on cellulose nanocrystals reinforced NR latex prepared by the solution casting method.[17]

To monitor the thiol−ene coupling reaction between thiols on the surface of m-CNCs and alkene groups in the molecules of natural rubber matrix, real-time FTIR analysis of the nanocomposites was performed under UV irradiation. The conversion of alkene groups to the thiol−ene addition products was determined from the change in absorbance of the band corresponding to =C−H out-of-plane bending at 836 $cm^{-1}$


DOI: 10.1021/acsami.5b03115
ACS Appl. Mater. Interfaces 2015, 7, 16303−16310

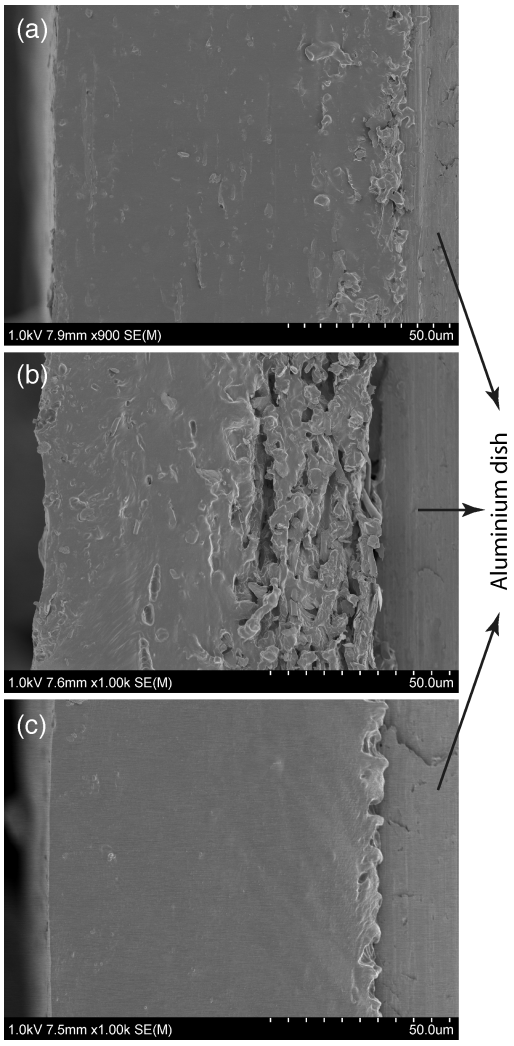


**Figure 2.** Typical FE-SEM micrographs showing the cross sections of the films of (a) NR/m-CNCs-10, (b) NR/CNCs-10, and (c) neat NR.

with respect to the irradiation time. As shown in Figure 3, the alkene conversion in pure NR and NR/CNCs nanocomposite

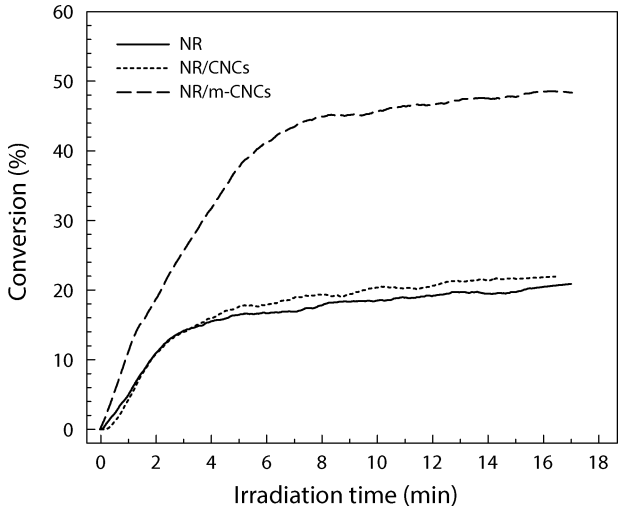


**Figure 3.** Real-time FTIR conversion profiles of the alkene groups in NR as a function of time.

reached 16% after 4 min of UV irradiation. This is probably due to the oxidation of alkene groups by hydroperoxides, formed as a result of UV irradiation in the presence of oxygen.[36] In the NR/m-CNCs sample, the alkene conversion reached 46% after 8 min of UV irradiation. The −SH groups present on the surface of m-CNCs reacted with the double bonds in natural rubber molecules forming thioether (C−S) bonds and resulted in a decrease of the ═C−H absorption band.

Figure 4 presents the cross-link density as determined by the Flory−Rehner equation as a function of CNCs content. The

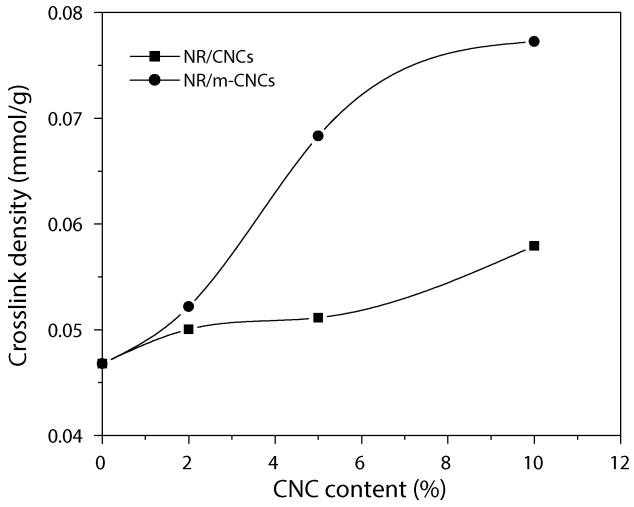


**Figure 4.** Cross-link density of NR/m-CNCs and NR/CNCs nanocomposites.

NR/m-CNCs nanocomposites showed a large increase in cross-link density compared to pure NR sample, especially at higher CNCs content. A cross-link density of 0.046 mmol/g observed in pure NR was due to a sparse amount of cross-linking due to the hydroperoxide groups formed upon UV irradiation, as revealed by real-time FTIR analysis. For the NR/CNCs nanocomposites, the cross-link density increased only slightly as compared to pure NR sample. The lower interfacial interaction between the polar CNCs and nonpolar NR matrix is ineffective in reducing the solvent uptake and swelling of the composite by keeping the polymer chains bound together. In contrast, m-CNCs are less polar and able to chemically cross-link natural rubber at the filler−matrix interface, thus making it more difficult for the solvent to permeate into the matrix.

From the above structural analysis results, it can be concluded that the thiol-modified CNCs, i.e., m-CNCs, were well dispersed in the NR matrix. The thiol−ene coupling reaction between the mercapto groups on the surface of CNCs and the alkene groups in NR provided effective chemical bonding at the filler−matrix interface, as illustrated in Figure 5.

**Uniaxial Tensile Tests.** The mechanical behavior of NR/CNCs and NR/m-CNCs nanocomposites was characterized by uniaxial tensile tests. Figure 6 shows the typical engineering stress−strain curves of the nanocomposites and the neat NR. Tensile properties of the composites are summarized in Table 1. The addition of unmodified CNCs in the NR matrix resulted in an increase in modulus and tensile strength as compared to the neat NR, while the strain-to-failure values of NR/CNCs composites were similar to that for the neat NR. At a CNCs content of 10 wt %, the modulus and tensile strength of the composite increased 73% and 75%, respectively. Such enhance-


DOI: 10.1021/acsami.5b03115
ACS Appl. Mater. Interfaces 2015, 7, 16303−16310

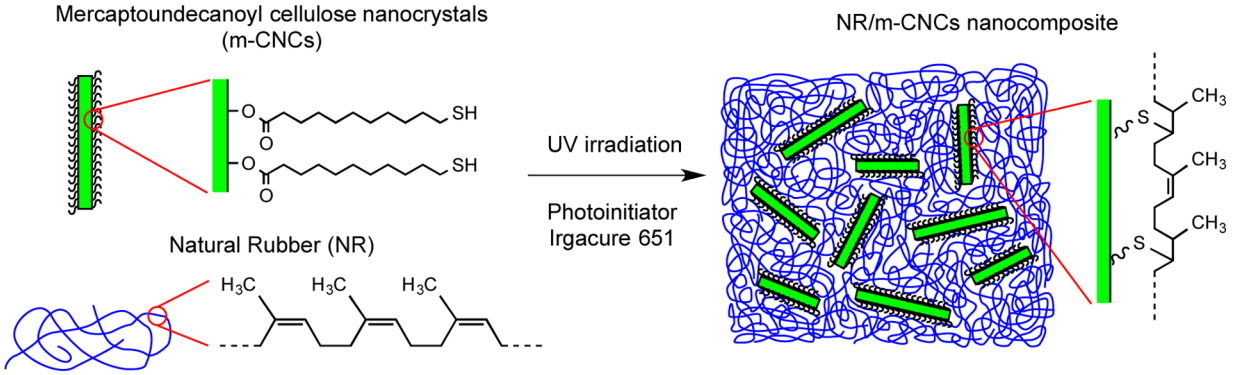


**Figure 5.** Illustration of the structure for the NR/m-CNCs nanocomposites.

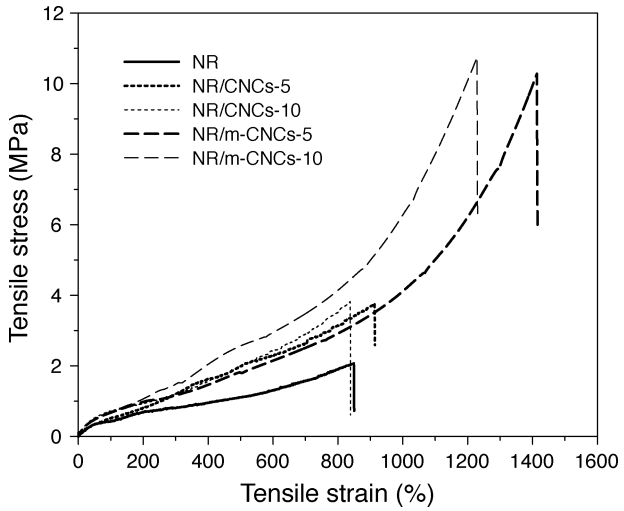


**Figure 6.** Tensile stress–strain curves of pure NR, NR/CNCs, and NR/m-CNCs. The designations 5 and 10 refer to weight fraction CNCs.

**Table 1. Tensile Properties of Modified and Unmodified Composites**

| | tensile strength (MPa) | strain-to-failure (%) | modulus (MPa) | work-of-fracture (MJ $m^{-3}$) |
|---|---|---|---|---|
| NR | 2.4 ± 0.4 | 910 ± 174 | 1.01 ± 0.08 | 1.45 ± 0.41 |
| NR/CNCs-2 | 3.3 ± 0.9 | 975 ± 120 | 1.05 ± 0.03 | 1.89 ± 0.67 |
| NR/CNCs-5 | 3.6 ± 0.4 | 960 ± 200 | 1.10 ± 0.08 | 1.73 ± 0.48 |
| NR/CNCs-10 | 4.2 ± 0.8 | 750 ± 125 | 1.75 ± 0.38 | 1.56 ± 0.32 |
| NR/m-CNCs-2 | 6.8 ± 1.5 | 1220 ± 30 | 1.49 ± 0.31 | 2.97 ± 0.39 |
| NR/m-CNCs-5 | 9.6 ± 2.0 | 1270 ± 157 | 1.53 ± 0.26 | 4.18 ± 0.75 |
| NR/m-CNCs-10 | 10.2 ± 1.3 | 1210 ± 110 | 1.86 ± 0.12 | 4.60 ± 0.57 |

ment is much lower than those observed previously by Bras et al.[37] and Bendahou et al.[17] for nonvulcanized natural rubber latex reinforced with cellulose whiskers from bagasse and date palm tree, respectively. This is due to the low aspect ratio of cotton CNCs compared to the ones isolated from date palm, and the agglomeration of CNCs in the NR matrix as solvent casted from an organic medium compared to the uniform dispersion using NR latex. For the NR/m-CNCs nanocomposites, significantly increased tensile strength and strain-to-failure were achieved compared to NR/CNCs composites. When comparing samples with the same content of CNCs (10 wt %), the tensile strength increased from 4.2 to 10.2 MPa, the strain-to-failure increased from 750% to 1210%, and the work-of-fracture value (toughness, proportional to area under stress–strain curve) increased almost 3 times (from 1.56 to 4.60 MJ $m^{-3}$) due to a more optimal combination of strength and strain to failure. The modulus of NR/m-CNCs-10 was 1.86 ± 0.12 MPa, similar to that for NR/CNCs-10 (1.75 ± 0.38 MPa). Although m-CNCs show better dispersion in the NR matrix, the fiber–fiber interaction between m-CNCs in the percolated m-CNCs network is weaker than the unmodified CNCs due to much fewer hydroxyl groups presented on the surface of m-CNCs compared to unmodified CNCs. Thus, the mechanical properties of the NR/CNCs composites at lower strains are mainly dependent on the volume fraction and the aspect ratio of the reinforcing filler, CNCs and m-CNCs. In NR/CNCs composites, the sparse cross-linking may not be sufficient at high strains. The interfacial interaction between the matrix and the nanocrystals may fail at higher strains creating voids in the composite which act as stress concentration points leading to composites fracture. The cross-linking through the thiol functionalities on the nanocrystal surface increases strength and toughness of the NR/m-CNCs composites as summarized in Table 1. Synergistic effect of cross-linking at the filler–matrix interface together with reinforcement in NR/m-CNCs nanocomposites offered by the thiol-modified CNCs nanocrystals is expressed in these results. In particular, a significant increase in strain-to-failure was obtained with m-CNCs, while a decrease in strain-to-failure was often observed in previous studies on NR/CNCs composites using NR latex.[17,19,37] Furthermore, when vulcanized natural rubber latex was reinforced with cellulose nanocrystals isolated from bamboo waste, the increase in tensile strength for 10 wt % composites compared to neat polymer was only 88%,[19] while in our case it is more than 320%.

**Dynamic Mechanical Thermal Analysis.** Figure 7 shows typical dynamic mechanical plots in the form of storage modulus ($E'$) and tan $\delta$ versus temperature for neat NR and NR/CNCs-5 and NR/m-CNCs-5 composites. At low temperature, $E'$ of neat NR and the composites remains at a glassy plateau up to a temperature approaching −50 °C. Both composites show higher $E'$ than neat NR. CNCs, both modified and unmodified, enhance the stiffness of the composites below the glass transition temperature where the segmental mobility of the polymer chains is restricted. At around −50 °C, both composites show a drop in modulus


DOI: 10.1021/acsami.5b03115
ACS Appl. Mater. Interfaces 2015, 7, 16303–16310

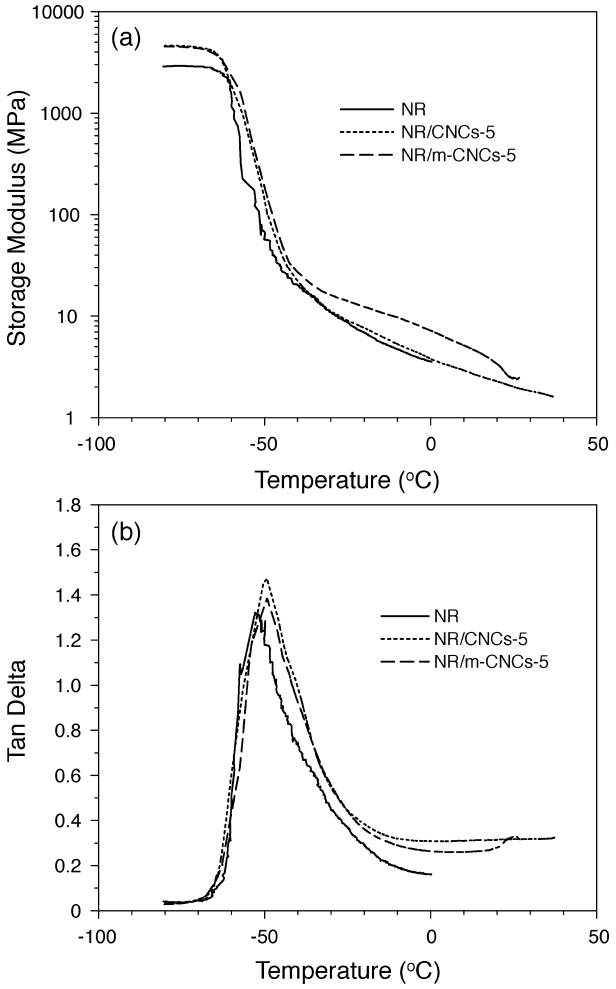


**Figure 7.** (a) Storage modulus ($E'$) and (b) tan $\delta$ as a function of temperature for neat NR and NR/CNCs-5 and NR/m-CNCs-5 nanocomposite films at 1 Hz.

corresponding to the glass transition region. Compared to the neat NR, both composites show transitions at higher temperature. Tan $\delta$ of the neat NR shows a maximum at −51.7 °C while for the composites it is −49 °C, showing a slight shift in the glass transition toward higher temperature; see Figure 7b. However, the difference of glass transition temperature between NR/m-CNCs-5 and NR/CNCs-5 is not significant. The cross-linking at the filler−matrix interphase in NR/m-CNCs composite is responsible for the improved modulus compared to NR/CNCs composite in the transition region. Effects of cross-linking are more apparent in the rubbery region giving further improvement in modulus. In general, Figure 7 indicates that the NR cross-link density in the present nanocomposites is fairly low, since cross-linking within the NR matrix (vulcanization) is not carried out. This work is really to prove the existence of covalent links at the NR/m-CNCs composite interface and to specifically study this effect. A more densely cross-linked NR network would have presented stronger CNCs reinforcement effects in the rubbery state.

**Stress Softening Effect.** When rubber vulcanizates are stretched and allowed to retract, subsequent extensions to the same strain may require lower stress. This stress softening behavior is termed Mullins effect.[38] Neat NR and NR/CNCs-5 and NR/m-CNCs-5 composites were therefore subjected to cyclic uniaxial tension with strain increasing 100% after each cycle to study stress softening in the composites. The resulting stress−strain curves of cyclic uniaxial tension are compared in Figure 8. When comparing NR/CNCs-5 composite with the

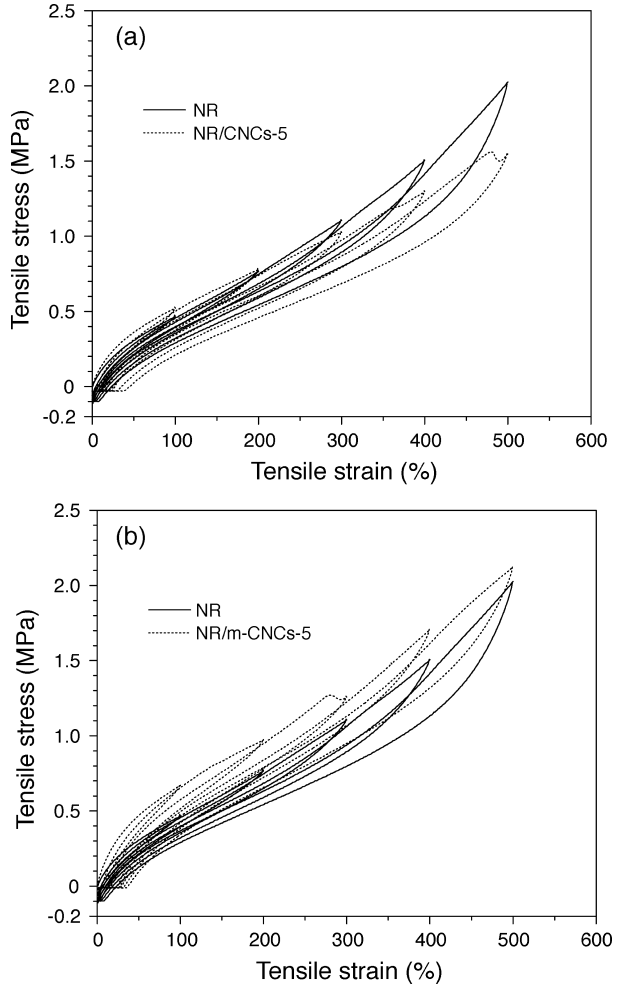


**Figure 8.** Stress−strain responses of (a) NR and NR/CNCs-5 and (b) NR and NR/m-CNCs-5 subjected to cyclic uniaxial tension with increasing maximum strain after every cycle.

neat NR sample (Figure 8a), the stress values at the end of the first two cycles are slightly higher for the NR/CNCs-5 sample. With increased strain, the resulting stress in the NR/CNCs-5 sample drops below that for the neat NR sample. This stress-softening is primarily due to two effects; chains fastened between adjacent filler particles are stretched to fracture, and the physical interaction between the unmodified CNCs and the natural rubber matrix is lost at high strain.[39] In contrast, for the NR/m-CNCs composites (Figure 8b), the covalent cross-linking bonds formed at the filler−matrix interface prevent loss of interface stress transfer and results in better preservation of stiffness even after several repeated loading cycles. Thus, the NR/m-CNCs nanocomposite consistently gives higher stress values than the neat NR elastomer even at high strain. When natural rubber was reinforced with carbon black and cross-linked with sulfur, the stress softening effect was around 20% in terms of stiffness loss,[40] which is much higher than the 3−5% in our case. The present concept reduces Mullins effect by combining stiff CNCs reinforcement with covalent links to the elastomer network through thiol-modified CNCs.


DOI: 10.1021/acsami.5b03115
ACS Appl. Mater. Interfaces 2015, 7, 16303−16310

## CONCLUSIONS

We have demonstrated a novel concept in biobased rubbery nanocomposites, i.e., the synergistic effect of using biobased nanoscale particles, in the form of cellulose nanocrystals, as reinforcing rod-like nanoparticles, which also have cross-linking sites for covalent coupling to the natural rubber elastomer network. Surface brush-modified m-CNCs bearing cross-linkable mercapto groups were successfully prepared by a simple esterification reaction on CNCs with 11-mercaptoundecanoic acid. The m-CNCs showed improved hydrophobicity and good dispersibility in organic solvent. Nanocomposite films with homogeneous dispersion of m-CNCs in the NR matrix were prepared by a solution casting method. The cross-link density of the NR/m-CNCs sample was confirmed to significantly increase with m-CNCs content. This is due to covalent cross-links formed at the filler−matrix interface via thiol−ene coupling reaction by UV irradiation. Such nanostructure is responsible for the remarkably improved mechanical properties of the composites. The NR/m-CNCs nanocomposite with 10 wt % of m-CNCs showed much higher values of engineering tensile strength (10.2 ± 1.3 MPa), strain-to-failure (1210 ± 110%), and toughness (4.60 ± 0.57 MJ $m^{-3}$) compared to pure NR and nanocomposites reinforced with unmodified CNCs. The NR/m-CNCs nanocomposites also showed much reduced stress softening effects (Mullins effect) since the CNCs were covalently linked to the NR network. As the present concept is general in material synthesis and design, we foresee the potential application of modified cellulose nanocrystals bearing thiols in the tire industry and general elastomeric composites. Note that the present experiments were designed to prove the effect of thiol-functional CNCs for covalent cross-linking at the NR/CNCs interface. If the NR network had been also cross-linked by traditional vulcanization mechanisms, the reinforcement effects would have been even stronger.

## AUTHOR INFORMATION

### Corresponding Author

*Tel: +46 8 5537 8383. Fax: +46 8 5537 8468. E-mail: qi@kth.se.

### Author Contributions

All authors have given approval to the final version of the manuscript.

### Notes

The authors declare no competing financial interest.

## ACKNOWLEDGMENTS

The authors are grateful to the Wallenberg Wood Science Center for financial support.

## REFERENCES

(1) Westlake, H. E. The Sulfurization of Unsaturated Compounds. *Chem. Rev.* **1946**, *39*, 219−239.
(2) Chandra, R.; Soni, R. K. Recent Developments in Thermally Curable and Photocurable Systems. *Prog. Polym. Sci.* **1994**, *19*, 137−169.
(3) Akiba, M.; Hashim, A. S. Vulcanization and Crosslinking in Elastomers. *Prog. Polym. Sci.* **1997**, *22*, 475−521.
(4) Karásek, L.; Sumita, M. Characterization of Dispersion State of Filler and Polymer-Filler Interactions in Rubber Carbon Black Composites. *J. Mater. Sci.* **1996**, *31*, 281−289.
(5) Hashim, A. S.; Azahari, B.; Ikeda, Y.; Kohjiya, S. The Effect of Bis(3-Triethoxysilylpropyl)Tetrasulfide on Silica Reinforcement of Styrene-Butadiene Rubber. *Rubber Chem. Technol.* **1998**, *71*, 289−299.
(6) Wang, M. J. Effect of Polymer-Filler and Filler-Filler Interactions on Dynamic Properties of Filled Vulcanizates. *Rubber Chem. Technol.* **1998**, *71*, 520−589.
(7) Kim, H.-Y.; Park, S. S.; Lim, S.-T. Preparation, Characterization and Utilization of Starch Nanoparticles. *Colloids Surf., B* **2015**, *126*, 607−620.
(8) Wu, Y. P.; Ji, M. Q.; Qi, Q.; Wang, Y. Q.; Zhang, L. Q. Preparation, Structure, and Properties of Starch/Rubber Composites Prepared by Co-Coagulating Rubber Latex and Starch Paste. *Macromol. Rapid Commun.* **2004**, *25*, 565−570.
(9) Bokobza, L. Multiwall Carbon Nanotube Elastomeric Composites: A Review. *Polymer* **2007**, *48*, 4907−4920.
(10) Vu, Y. T.; Mark, J. E.; Pham, L. H.; Engelhardt, M. Clay Nanolayer Reinforcement of Cis-1,4-Polyisoprene and Epoxidized Natural Rubber. *J. Appl. Polym. Sci.* **2001**, *82*, 1391−1403.
(11) Varghese, S.; Karger-Kocsis, J. Natural Rubber-Based Nanocomposites by Latex Compounding with Layered Silicates. *Polymer* **2003**, *44*, 4921−4927.
(12) Karger-Kocsis, J.; Wu, C. M. Thermoset Rubber/Layered Silicate Nanocomposites. Status and Future Trends. *Polym. Eng. Sci.* **2004**, *44*, 1083−1093.
(13) Abdul Khalil, H. P. S.; Davoudpour, Y.; Islam, M. N.; Mustapha, A.; Sudesh, K.; Dungani, R.; Jawaid, M. Production and Modification of Nanofibrillated Cellulose Using Various Mechanical Processes: A Review. *Carbohydr. Polym.* **2014**, *99*, 649−665.
(14) Qing, Y.; Sabo, R.; Zhu, J. Y.; Agarwal, U.; Cai, Z. Y.; Wu, Y. Q. A Comparative Study of Cellulose Nanofibrils Disintegrated Via Multiple Processing Approaches. *Carbohydr. Polym.* **2013**, *97*, 226−234.
(15) Pasquini, D.; Teixeira, E. D.; Curvelo, A. A. D.; Belgacem, M. N.; Dufresne, A. Extraction of Cellulose Whiskers from Cassava Bagasse and Their Applications as Reinforcing Agent in Natural Rubber. *Ind. Crops Prod.* **2010**, *32*, 486−490.
(16) Siqueira, G.; Tapin-Lingua, S.; Bras, J.; da Silva Perez, D.; Dufresne, A. Mechanical Properties of Natural Rubber Nanocomposites Reinforced with Cellulosic Nanoparticles Obtained from Combined Mechanical Shearing, and Enzymatic and Acid Hydrolysis of Sisal Fibers. *Cellulose* **2011**, *18*, 57−65.
(17) Bendahou, A.; Habibi, Y.; Kaddami, H.; Dufresne, A. Physico-Chemical Characterization of Palm from *Phoenix Dactylifera*-L, Preparation of Cellulose Whiskers and Natural Rubber-Based Nanocomposites. *J. Biobased Mater. Bioenergy* **2009**, *3*, 81−90.
(18) Abraham, E.; Deepa, B.; Pothan, L. A.; John, M.; Narine, S. S.; Thomas, S.; Anandjiwala, R. Physicomechanical Properties of Nanocomposites Based on Cellulose Nanofibre and Natural Rubber Latex. *Cellulose* **2013**, *20*, 417−427.
(19) Visakh, P. M.; Thomas, S.; Oksman, K.; Mathew, A. P. Crosslinked Natural Rubber Nanocomposites Reinforced with Cellulose Whiskers Isolated from Bamboo Waste: Processing and Mechanical/Thermal Properties. *Composites, Part A* **2012**, *43*, 735−741.
(20) Gao, Tian Ming; Huang, M. F.; Xie, Rui Hong; Chen, Hong Lian Preparation and Characterization of Nanocrystalline Cellulose/Natural Rubber (Ncc/Nr) Composites. *Adv. Mater. Res.* **2013**, *712−715*, 111−114.
(21) Rosilo, H.; Kontturi, E.; Seitsonen, J.; Kolehmainen, E.; Ikkala, O. Transition to Reinforced State by Percolating Domains of Intercalated Brush-Modified Cellulose Nanocrystals and Poly(Butadiene) in Cross-Linked Composites Based on Thiol-Ene Click Chemistry. *Biomacromolecules* **2013**, *14*, 1547−1554.
(22) Hoyle, C. E.; Bowman, C. N. Thiol-Ene Click Chemistry. *Angew. Chem., Int. Ed.* **2010**, *49*, 1540−1573.
(23) Claudino, M.; Mathevet, J. M.; Jonsson, M.; Johansson, M. Bringing D-Limonene to the Scene of Bio-Based Thermoset Coatings Via Free-Radical Thiol-Ene Chemistry: Macromonomer Synthesis, Uv-


DOI: 10.1021/acsami.5b03115
*ACS Appl. Mater. Interfaces* 2015, 7, 16303−16310

Curing and Thermo-Mechanical Characterization. *Polym. Chem.* **2014**, *5*, 3245−3260.
(24) Claudino, M.; Jonsson, M.; Johansson, M. Utilizing Thiol-Ene Coupling Kinetics in the Design of Renewable Thermoset Resins Based on D-Limonene and Polyfunctional Thiols. *RSC Adv.* **2014**, *4*, 10317−10329.
(25) Claudino, M.; Jonsson, M.; Johansson, M. Thiol-Ene Coupling Kinetics of D-Limonene: A Versatile 'Non-Click' Free-Radical Reaction Involving a Natural Terpene. *RSC Adv.* **2013**, *3*, 11021−11034.
(26) Goetz, L.; Mathew, A.; Oksman, K.; Gatenholm, P.; Ragauskas, A. J. A Novel Nanocomposite Film Prepared from Crosslinked Cellulosic Whiskers. *Carbohydr. Polym.* **2009**, *75*, 85−89.
(27) Goetz, L.; Foston, M.; Mathew, A. P.; Oksman, K.; Ragauskas, A. J. Poly(Methyl Vinyl Ether-Co-Maleic Acid)-Polyethylene Glycol Nanocomposites Cross-Linked in Situ with Cellulose Nanowhiskers. *Biomacromolecules* **2010**, *11*, 2660−2666.
(28) Pei, A. H.; Malho, J. M.; Ruokolainen, J.; Zhou, Q.; Berglund, L. A. Strong Nanocomposite Reinforcement Effects in Polyurethane Elastomer with Low Volume Fraction of Cellulose Nanocrystals. *Macromolecules* **2011**, *44*, 4422−4427.
(29) Zhou, Q.; Brumer, H.; Teeri, T. T. Self-Organization of Cellulose Nanocrystals Adsorbed with Xyloglucan Oligosaccharide-Poly(Ethylene Glycol)-Polystyrene Triblock Copolymer. *Macromolecules* **2009**, *42*, 5430−5432.
(30) Park, S. Y.; Chung, J. W.; Priestley, R. D.; Kwak, S. Y. Covalent Assembly of Metal Nanoparticles on Cellulose Fabric and Its Antimicrobial Activity. *Cellulose* **2012**, *19*, 2141−2151.
(31) Ellman, G. L. A Colorimetric Method for Determining Low Concentrations of Mercaptans. *Arch. Biochem. Biophys.* **1958**, *74*, 443−450.
(32) Flory, P. J.; Rehner, J. Statistical Mechanics of Cross-Linked Polymer Networks II. Swelling. *J. Chem. Phys.* **1943**, *11*, 521−526.
(33) Chaudhuri, D. K. R.; Hermans, J. J. Grafting onto Cellulosic Macromolecules through Chain Transfer to Mercaptoethyl Side Chains. I. Experimental Procedure and Results. *J. Polym. Sci.* **1960**, *48*, 159−166.
(34) Aoki, D.; Teramoto, Y.; Nishio, Y. Sh-Containing Cellulose Acetate Derivatives: Preparation and Characterization as a Shape Memory-Recovery Material. *Biomacromolecules* **2007**, *8*, 3749−3757.
(35) Ashraf, S.; Saif-ur-Rehman; Sher, F.; Khalid, Z. M.; Mehmood, M.; Hussain, I. Synthesis of Cellulose-Metal Nanoparticle Composites: Development and Comparison of Different Protocols. *Cellulose* **2014**, *21*, 395−405.
(36) Gonon, L.; Gardette, J. L. Photooxidation Mechanism of Styrene-Isoprene Copolymer: Evolution of the Profile of Oxidation According to the Composition. *Polymer* **2000**, *41*, 1669−1678.
(37) Bras, J.; Hassan, M. L.; Bruzesse, C.; Hassan, E. A.; El-Wakil, N. A.; Dufresne, A. Mechanical, Barrier, and Biodegradability Properties of Bagasse Cellulose Whiskers Reinforced Natural Rubber Nanocomposites. *Ind. Crops Prod.* **2010**, *32*, 627−633.
(38) Diani, J.; Fayolle, B.; Gilormini, P. A Review on the Mullins Effect. *Eur. Polym. J.* **2009**, *45*, 601−612.
(39) Bueche, F. Molecular Basis for the Mullins Effect. *J. Appl. Polym. Sci.* **1960**, *4*, 107−114.
(40) Harwood, J. A. C.; Mullins, L.; Payne, A. R. Stress Softening in Natural Rubber Vulcanizates. Part II. Stress Softening Effects in Pure Gum and Filler Loaded Rubbers. *J. Appl. Polym. Sci.* **1965**, *9*, 3011−3021.


DOI: 10.1021/acsami.5b03115
*ACS Appl. Mater. Interfaces* 2015, 7, 16303−16310